A&A 615, A165 (2018)
https://doi.org/10.1051/0004-6361/201832695

Astronomy & Astrophysics

Chemical composition of giant stars in the open cluster IC 4756⋆,⋆⋆

Vilius Bagdonas[1], Arnas Drazdauskas[1], Gražina Tautvaišienė[1], Rodolfo Smiljanic[2], and Yuriy Chorniy[1]

[1] Institute of Theoretical Physics and Astronomy, Vilnius University, Saulėtekio al. 3, 10257 Vilnius, Lithuania
e-mail: vilius.bagdonas@ff.vu.lt
[2] Nicolaus Copernicus Astronomical Center, Polish Academy of Sciences, Bartycka 18, 00-716 Warsaw, Poland

Received 24 January 2018 / Accepted 29 March 2018

ABSTRACT

Context. Homogeneous investigations of red giant stars in open clusters contribute to studies of internal evolutionary mixing processes inside stars, which are reflected in abundances of mixing-sensitive chemical elements like carbon, nitrogen, and sodium, while α- and neutron-capture element abundances are useful in tracing the Galactic chemical evolution.
Aims. The main aim of this study is a comprehensive chemical analysis of red giant stars in the open cluster IC 4756, including determinations of $^{12}C/^{13}C$ and C/N abundance ratios, and comparisons of the results with theoretical models of stellar and Galactic chemical evolution.
Methods. We used a classical differential model atmosphere method to analyse high-resolution spectra obtained with the FEROS spectrograph on the 2.2 m MPG/ESO Telescope. The carbon, nitrogen, and oxygen abundances, $^{12}C/^{13}C$ ratios, and neutron-capture element abundances were determined using synthetic spectra, and the main atmospheric parameters and abundances of other chemical elements were determined from equivalent widths of spectral lines.
Results. We have determined abundances of 23 chemical elements for 13 evolved stars and $^{12}C/^{13}C$ ratios for six stars of IC 4756. The mean metallicity of this cluster, as determined from nine definite member stars, is very close to solar – [Fe/H] = -0.02 ± 0.01. Abundances of carbon, nitrogen, and sodium exhibit alterations caused by extra-mixing: the mean $^{12}C/^{13}C$ ratio is lowered to 19 ± 1.4, the C/N ratio is lowered to 0.79 ± 0.05, and the mean [Na/Fe] value, corrected for deviations from the local thermodynamical equilibrium encountered, is enhanced by 0.14 ± 0.05 dex. We compared our results to those by other authors and theoretical models.
Conclusions. Comparison of the α-element results with the theoretical models shows that they follow the thin disc α-element trends. Being relatively young (~800 Myr), the open cluster IC 4756 displays a moderate enrichment of *s*-process-dominated chemical elements compared to the Galactic thin disc model and confirms the enrichment of *s*-process-dominated elements in young open clusters compared to the older ones. The *r*-process-dominated element europium abundance agrees with the thin disc abundance. From the comparison of our results for mixing-sensitive chemical elements and the theoretical models, we can see that the mean values of $^{12}C/^{13}C$, C/N, and [Na/Fe] ratios lie between the model with only the thermohaline extra-mixing included and the model which also includes the rotation-induced mixing. The rotation was most probably smaller in the investigated IC 4756 stars than 30% of the critical rotation velocity when they were on the main sequence.

Key words. stars: abundances – open clusters and associations: individual: IC 4756 – stars: horizontal-branch – stars: evolution

1. Introduction

Our Galaxy has always occupied an important place in the field of astrophysics. In today's era of space- and ground-based surveys like *Gaia* (Gaia Collaboration 2016), *Gaia*-ESO (Gilmore et al. 2012), APOGEE (Nidever et al. 2012), GALAH (De Silva et al. 2015), and RAVE (Kunder et al. 2017), there is an abundance of data for studying the formation and evolution of the Milky Way. However, even massive surveys do not include every object, or every aspect of selected objects. That is why employing smaller telescopes and individual observations of selected targets is still important, providing valuable information that is otherwise lost due to various constraints that are often present in massive surveys. In this paper, we continue our investigation of red giant branch stars in open clusters from high-resolution spectra by analysing the open cluster IC 4756.

Stars in open clusters are known to be born from the same molecular cloud at roughly the same time and distance. Sharing the same primordial material, the open cluster stars have similar metallicity and chemical composition. New open clusters are constantly identified and the available sample of these stellar associations expands in variety of ages, heliocentric and galactocentric distances, and metallicities. Stars in open clusters have a significant advantage over the field stars. Precise ages that can be determined for open clusters allow studies of how the properties of the Galactic disc, such as chemical patterns for example, change with time, providing important constraints for Galactic modelling. Furthermore, while members of open clusters have a common origin, they still have a different initial mass, which predetermines the lifetime of a star. For this reason, stars in open clusters are crucial tools in understanding how photospheric chemical composition varies due to stellar evolutionary effects.

Every chemical element in stellar atmospheres provides valuable information. Some of them, such as carbon and nitrogen

⋆ Based on observations collected at the European Organization for Astronomical Research in the Southern Hemisphere under ESO programme 085.D-0093(A).
⋆⋆ The full Table 2 is only available at the CDS via anonymous ftp to cdsarc.u-strasbg.fr (130.79.128.5) or via http://cdsarc.u-strasbg.fr/viz-bin/qcat?J/A+A/615/A165

as investigated in this work, being susceptible to stellar evolutionary effects, show alterations of their observable abundances in photospheres of evolved stars. The standard stellar evolution model only predicts one mixing event on the red giant branch (RGB) – called the first dredge-up (Iben 1965), when the convective envelope expands and connects the inner layers containing the nuclear processed material and allows it to rise to the surface. However, as observational evidence suggests (Smiljanic et al. 2009; Mikolaitis et al. 2010, 2011a,b; Drazdauskas et al. 2016a,b; Tautvaišienė et al. 2016 and references therein), after the luminosity bump on the RGB, there is a further decrease of ^{12}C and increase of ^{14}N in low-mass stars, which cannot be explained by standard stellar evolution models. For example, in stars of solar metallicity and about 2.5 solar mass, the carbon abundance may decrease by 0.3 dex, and the nitrogen abundance may increase by 0.3 dex (Charbonnel & Lagarde 2010). The exact causes of this effect are not yet fully understood and there are models which predict different extra-mixing effects depending on stellar turn-off mass and metallicity (Chanamé et al. 2005; Charbonnel 2006; Cantiello & Langer 2010; Charbonnel & Lagarde 2010; Denissenkov 2010; Lagarde et al. 2011, 2012; Wachlin et al. 2011; Angelou et al. 2012; Lattanzio et al. 2015).

In recent years there has been an increase in studies of carbon and nitrogen in field and open cluster stars. Together with theoretical models (Charbonnel & Lagarde 2010; Lagarde et al. 2012) we try to constrain possible mechanisms governing the extra-mixing in evolved stars. In our work, in addition to carbon and nitrogen ratios, we look at carbon isotopic ratios (^{12}C/^{13}C), which are less susceptible to systematic errors in stellar atmospheric parameters and provide an even better insight into the extra-mixing phenomenon.

Abundances of other chemical elements like oxygen and α- and iron-peak elements play an important role when trying to constrain theoretical models of Galactic chemical evolution. Oxygen and α-elements are mainly produced via Type II supernovae explosions and the timescales of elemental injection into the interstellar medium are short. Fe-peak elements, produced by Type Ia supernovae, on the other hand, have longer interstellar medium enrichment timescales (Tinsley 1979; Matteucci & Greggio 1986; Wyse & Gilmore 1988; Yong et al. 2005). As [Fe/H] and [α/Fe] steadily increase and decrease over time, respectively, the ratios of these elements are good age or place-of-birth indicators of specific objects of the Galaxy (Matteucci 1992). It is also established that the scatter of abundances of [α/Fe] at the same [Fe/H] value can help us distinguish between thin and thick discs (Mikolaitis et al. 2014; Masseron & Gilmore 2015).

Abundances of neutron-capture (n-capture) chemical elements also deserve further investigations. A recent study of low-mass stars by D'Orazi et al. (2009) showcased an interesting phenomenon: the abundance of the slow neutron capture process (*s*-process) element barium seems to increase with decreasing cluster age. The barium abundances for young open clusters exhibited the enhancements up to ~0.6 dex. While later studies confirmed this finding for barium, to the same or a lesser extent, the abundance enrichment patterns for other *s*-process elements in young open clusters are still debatable (e.g. Maiorca et al. 2011; Yong et al. 2012; D'Orazi et al. 2012; Jacobson & Friel 2013; Mishenina et al. 2013, 2015; Reddy & Lambert 2015; D'Orazi et al. 2017). The suggested explanations for higher *s*-process element yields include higher production rates of these elements than previously thought by very old, low-mass AGB stars (e.g. Maiorca et al. 2011), additional contribution by the *i*-process (Mishenina et al. 2015), or overestimation of barium abundances by a standard LTE abundance analysis (Reddy & Lambert 2017). Overall, a comparison of n-capture chemical element abundances not only with age, but with other important parameters such as metallicity or galactocentric distance (e.g. Jacobson & Friel 2013; Overbeek et al. 2016) provides important information about stellar evolution and about the Galaxy as a whole.

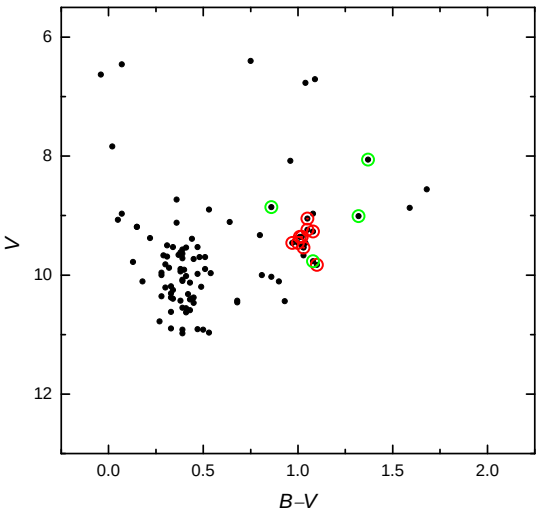

Fig. 1. Colour-magnitude diagram of the open cluster IC 4756. The *UBV* photometry of the open cluster is from Alcaino (1965). The stars investigated in this work are marked with circles. The green circles represent the stars with uncertain membership status.

We compare our results with theoretical models, which depict aspects of both Galactic and stellar chemical evolution. Models by Magrini et al. (2009), Pagel & Tautvaisiene (1997), and Maiorca et al. (2012) trace the Galactic evolution as a function of the galactocentric distance, metallicity, and age, respectively, whereas models by Lagarde et al. (2012) provide insight into the stellar evolution and alterations of light elements in atmospheres of evolved stars.

2. Cluster IC 4756

IC 4756 is a relatively young open cluster in our Galaxy. Like most young open clusters, IC 4756 is located in the inner part of the Galactic disc (the galactic coordinates l = 36°.381, b = 5°.242), at a galactocentric distance R_{gc} of around 8.1 kpc (Gilroy 1989). In order to separate cluster members from field stars, the first photometric study for this cluster was made by Kopff (1943), and later by Alcaino (1965), Seggewiss (1968), and Herzog et al. (1975). There are several cluster age determinations: an age of 0.82 Gyr was derived by Alcaino (1965), 0.8 Gyr by Gilroy (1989), 0.79 Gyr by Salaris et al. (2004), 0.8 ± 0.2 Gyr by Pace et al. (2010), and most recently 0.89 ± 0.07 Gyr was determined by Strassmeier et al. (2015).

There are a few studies of this cluster in which metallicity was determined from photometry. Smith (1983), using a *DDO* cyanogen colour excess parameter, calculated the cluster metallicity [Fe/H] = 0.04 ± 0.05. The most recent comprehensive study of this cluster was made by Strassmeier et al. (2015). In their work, an averaged metallicity from several CMD diagrams was −0.03 ± 0.02 dex and a combined metallicity from spectroscopy and photometry was −0.08 ± 0.06 dex.

Gilroy (1989), using high-resolution spectroscopy from seven giant stars, determined a cluster metallicity [Fe/H] = 0.04 ± 0.07. In a later study of this cluster performed by (Luck 1994),

Table 1. Analysed stars and their parameters.

ID	RA(2000) deg	Dec(2000) deg	V mag	$B-V$ mag	Date Obs.	Exp. time seconds	Rad. vel. km s^{-1}	S/N (at ~6400 Å)
12	278.9476	+5.3381	9.54	1.03	2010-06-28	600	−25.25	~140
14	278.9936	+5.4167	8.86	0.86	2010-06-30	600	−24.82	~180
28	279.1384	+5.2119	9.01	1.32	2010-06-30	600	−25.26	~160
38	279.2717	+5.2921	9.83	1.10	2010-06-27	900	−25.78	~140
42	279.3365	+5.8953	9.46	0.97	2010-06-30	600	−24.92	~140
44	279.3762	+5.2044	9.77	1.08	2010-06-30	900	−25.00	~140
52	279.3992	+5.2605	8.06	1.37	2010-06-30	120	−25.21	~120
69	279.5215	+5.4094	9.24	1.05	2010-06-27	600	−27.70	~150
81	279.5865	+5.4340	9.46	1.00	2010-06-30	600	−23.25	~140
101	279.6824	+5.2389	9.36	1.02	2010-06-30	600	−24.70	~140
109	279.7205	+5.3379	9.05	1.05	2010-06-30	300	−25.25	~120
125	279.8245	+5.2302	9.36	1.01	2010-06-30	600	−24.00	~140
164	280.0771	+5.3144	9.27	1.08	2010-06-30	600	−25.51	~150

Notes. The IDs are adopted from Kopff (1943), the UBV photometry are taken from Alcaino (1965), the radial velocities as determined in this work.

four giant stars gave a metallicity [Fe/H] = −0.03 ± 0.05. Slightly sub-solar metallicities of [Fe/H] = −0.22 ± 0.12 (8 stars) and [Fe/H] = −0.15 ± 0.04 (6 stars) were derived using moderate-resolution CCD spectra by Thogersen et al. (1993) and Jacobson et al. (2007), respectively. A later study by Twarog et al. (1997), using the *DDO* photometry from Smith (1983) and data from Thogersen et al. (1993), provided the weighted average metallicity of −0.06 ± 0.10 dex. The recent study by Smiljanic et al. (2009) determined metallicities of 0.04 ± 0.03 dex. It is worth mentioning that Santos et al. (2009), using a line-list by Sousa et al. (2008), determined metallicity of 0.02 ± 0.02 dex, while for the same stars a value of [Fe/H] = 0.08 ± 0.01 was obtained using a line-list by Hekker & Meléndez (2007). The most recent entirely spectroscopic study of 12 giant stars in this cluster was published by Ting et al. (2012), in which a metallicity of −0.01 ± 0.1 dex was determined.

However, these works investigated relatively small samples of stars and were mostly dedicated to α- and iron-peak chemical elements. A more comprehensive study of C, N, and O abundances is required, as these abundances were previously determined only by Smiljanic et al. (2009) for three stars, and an upper value of oxygen abundance was evaluated also from three stars by Pace et al. (2010). The $^{12}C/^{13}C$ ratios for this cluster were also derived only by Gilroy (1989) and Smiljanic et al. (2009). A deeper analysis for the n-capture elements is also needed. The only determinations of abundances for these elements were performed by Luck (1994; Ba, Y, Zr, Nd, and Eu abundances presented), by Maiorca et al. (2011; provided abundances of Y, Zr, La, Ce) and by Ting et al. (2012; abundances of only Ba determined). Thus, the deficiency of studies of neutron capture elements for this cluster and also its young age, make IC 4756 the important object to analyse when trying to constrain s- and r-process element enrichment patterns in young ages.

3. Observations and method of analysis

3.1. Observations

The spectra of our programme stars were observed using the bench-mounted, high-resolution astronomical echelle spectrograph Fiber-Fed Extended Range Optical Spectrograph (FEROS; Kaufer et al. 1999) at the 2.2 m MPG/ESO Telescope in La Silla, between June 27 and 30, 2010. The FEROS covers a whole visible range of 3500–9200 Å over 39 orders with the resolving power of about 48 000. The FEROS Data Reduction System pipeline within MIDAS was used for spectral reductions. Depending on magnitudes of the observed objects, exposure times where chosen to achieve signal-to-noise ratios (S/Ns) higher than 120 at about 6400 Å. The most luminous object was observed for 120 s, while others have observation times ranging from 300 to 600 s with a maximum of 900 s. A total of 13 stars in the cluster IC 4756 were observed. We list them in Table 1. The identifications of stars were adopted from Kopff (1943). A total of 13 stars in the cluster IC 4756 were observed (Fig. 1).

3.2. Membership

The red giants analysed here were selected for observations based on the results of the radial velocity monitoring programme of Mermilliod et al. (2008). All the 13 giants in our sample were considered to be likely cluster members. Moreover, all were found to be single stars, apart of star 69 which is a single lined spectroscopic binary. Mermilliod et al. (2008) found a mean radial velocity of −25.16 ± 0.25 (error) ±1.10 (rms) km s^{-1} for IC 4756. Recently, Casamiquela et al. (2016) reported a mean radial velocity of −24.7 ± 0.7 km s^{-1} for the cluster based on the analysis of 7 red giants. The radial velocities determined in our work are within 2 σ (rms) of these two mean values for all 12 single giants of the sample. Therefore, as far as radial velocities are concerned, there is no reason to doubt the membership of any of the giants that were observed.

Star 69 is a system with a long period of 1994 days, and a very circular orbit, with eccentricity of 0.05 (Mermilliod et al. 2007; Van der Swaelmen et al. 2017). It was included in the sample analysed here to follow up on the results of Smiljanic et al. (2009), who found star 69 to have very different C and N abundances with respect to other cluster giants (in fact, only limits were determined: [C/Fe] ≤ −0.60 and [N/Fe] ≥ +0.55). As suggested in Smiljanic et al. (2009), and further discussed in Van der Swaelmen et al. (2017), star 69 is likely a post-mass-transfer system.

Membership probabilities based on proper motions from UCAC4 (Zacharias et al. 2013) have been determined for stars in IC 4756 by Dias et al. (2014) and Sampedro et al. (2017). Stars 69,

81, 101, 109, and 125 are part of the Dias et al. (2014) catalogue and all five have membership probability of 99%. Only stars 81 and 109, are part of the Sampedro et al. (2017) catalogue. The two have very high membership probabilities (>95%) according to all three methods used in that work.

Six of our sample giants were included in the work of Frinchaboy & Majewski (2008). These authors determined membership probabilities using *Tycho*-2 proper motions, radial velocities and considering the spatial distribution of the stars. Four stars were considered to be members of the cluster (stars 69, 81, 101, and 109) while stars 44 and 52 (TYC 455-00950-1 and TYC 455-00136-1) were found to be non-members (with membership probabilities of 13% and 47%, respectively).

Two of our stars (numbers 14 and 109) were included in a sample analysed by Baumgardt et al. (2000). These authors determined membership probabilities for stars in open clusters using HIPPARCOS parallaxes and proper motions combined with ground-based data (photometry, radial velocity, proper motion, distance from the cluster centre). The membership probabilities determined by Baumgardt et al. (2000) for stars 14 and 109 were 59% and 80%, respectively.

Another work determining membership probabilities for stars in IC 4756 was conducted by Herzog et al. (1975) using proper motions. Ten of our sample giants were included in that work (all except stars 12, 14, and 42). Only stars 28 and 52 were found to be non-members with membership probabilities of 0% and 29%, respectively. For star 44, Herzog et al. (1975) found a membership probability of 96%, which disagrees with the 13% probability found by Frinchaboy & Majewski (2008) using the *Tycho*-2 data; the latter probably being more robust. For star 14, the only available study (Baumgardt et al. 2000) indicates a somewhat low membership probability. Stars 12 and 42 were not included in any of the membership works that used proper motions mentioned here.

Summarizing, there seems to be some evidence that stars 14, 28, 44, and 52 might be non-members of the cluster. In this work, we check how their chemical composition agrees with composition of the high-probability members of the cluster.

3.3. Atmospheric parameters and elemental abundances

We used a standard spectroscopic method, differential to the Sun, for the determination of atmospheric parameters. Effective temperatures ($T_{\rm eff}$) were derived by minimizing a slope between abundances of Fe I lines with different lower-level excitation potentials (χ). The step of our $T_{\rm eff}$ determination was 5 K, which corresponds to the slope change d [Fe/H]/d EP = 0.001. Surface gravities ($\log g$) were determined using the iron ionization equilibrium. Since our step in $\log g$ determination was 0.1, we allowed abundances of Fe I and Fe II to differ by no more than 0.02 dex. The final iron abundance was based on the neutral iron lines. In order to find microturbulence velocities ($v_{\rm t}$), a minimization of scatter in abundances from Fe I lines was employed, as well as minimization of the iron abundance trend with regard to the Fe I line equivalent widths (EWs). Equivalent widths of about 35–38 Fe I and 4–5 Fe II lines were used for the derivation of stellar metallicities, as well as other atmospheric parameters. For the measurement of EWs, we used a SPLAT-VO programme package (Škoda et al. 2014).

The EQWIDTH and BSYN software packages (developed at the Uppsala Observatory) were used to derive elemental abundances from EWs and synthetic spectra, respectively. We have taken a set of plane-parallel, one-dimensional, hydrostatic, constant flux local thermodynamical equilibrium (LTE) model atmospheres (Gustafsson et al. 2008) from the MARCS stellar model atmosphere and flux library[1]. Atomic oscillator strengths for the main lines used in this work were taken from the inverse solar spectrum analysis performed by Gurtovenko & Kostyk (1989). Using the gf values and solar EWs from Gurtovenko & Kostyk (1989), we computed the solar elemental abundances used for the differential determination of elemental abundances in the programme stars. For the Sun, we used the main atmospheric parameters $T_{\rm eff}$ = 5777 K, $\log g$ = 4.44, and the microturbulent velocity value 0.8 km s^{-1}, as in our earlier studies (e.g. Tautvaišienė et al. 2000) where the same method of analysis was applied.

Abundances of Na, Mg, Al, Si, Ca, Sc, Ti, Cr, and Ni were determined using the EWs method. The EWs of spectral lines are presented in an online table (see Table 2 for an example). The number of lines for each element slightly varied among the stars, as every line was inspected individually and some of them were excluded due to contamination of cosmic rays or other observational effects. For sodium, we applied non-LTE (NLTE) corrections as described by Lind et al. (2011). The corrections range from −0.08 to −0.11 dex.

The spectral synthesis method was used to derive C, N, and O, as well as neutron-capture element abundances. We used the forbidden line at 6300.3 Å for the oxygen abundance determination. The gf values for ^{58}Ni and ^{60}Ni isotopic line components, which blend the oxygen line, were taken from Johansson et al. (2003). Two C_2 molecular bands at 5135 and 5635 Å were used to determine carbon abundances and up to eight ^{12}CN molecular lines in the region of 7980–8005 Å for the nitrogen abundances. We used the same molecular data of C_2 as in Gonzalez et al. (1998) and the CN molecular data provided by Bertrand Plez. The Vienna Atomic Line Data Base (VALD; Piskunov et al. 1995) was used for preparation of input data used in the calculations. In order to check correctness of the input data, synthetic spectra of the Sun were compared to the solar atlas of Kurucz (2005) with solar abundances of (Grevesse & Sauval 2000) and necessary adjustments were made to the line atomic data.

Since carbon and oxygen are bound together by the molecular equilibrium, in order to correctly measure abundances of these elements, we investigated them in unison. How abundance changes in one of the elements affect abundances in the others is shown in Table 3. As we can see, the most sensitive case is between nitrogen and carbon, where 0.1 dex change in carbon coincides with a change in the nitrogen abundance by the same amount. We adopt a procedure of a few back and forth iterations between these elements to achieve a combination of these three abundances, until all of them match the features in the observed spectra.

The synthetic spectra method was also used for the determination of (Mn, Co, Y, Zr, Ba, La, Ce, Pr, Nd, and Eu abundances. Cobalt abundances were determined from the 5280.62, 5301.03, 5352.05, 5530.78, 5647.23, 6188.98, 6455, and 6814.95 Å lines. For the analysis of lines at 5301.03 and 5530.78 Å we applied hyperfine structure (HFS) data from Nitz et al. (1999), while for the remaining Co I lines the HFS data were taken from Cardon et al. (1982). Manganese was investigated using lines at 6013.49, 6016.64, and 6021.80 Å with the HFS data taken from Den Hartog et al. (2011). Yttrium abundances were determined from the Y II lines at 4883.69, 4900.12, 4982.14, 5200.41, and 5402.78 Å; zirconium from the Zr I lines at 5385.10 and 6127.50 Å; lanthanum from the La II lines at 5123.01, 6320.41,

[1] http://marcs.astro.uu.se/

Table 2. Spectral line equivalent widths in stars of IC 4756.

Elem.	Wavelength	EW (mÅ)												
	(Å)	12	14	28	38	42	44	52	69	81	101	109	125	164
Na I	5148.84	33	51	42	–	32	31	52	40	30	35	39	28	33
	6154.22	67	91	93	67	71	68	107	78	65	68	80	69	74
	6160.75	89	110	109	85	87	85	123	93	81	84	94	89	94
Mg I	6318.70	55	67	67	56	55	53	70	55	46	54	57	55	61
...	...	...	...	...	...	...	...	...	...	...	...	...	...	...

Notes. The full table is available at the CDS.

Table 3. Effects on derived abundances and isotopic ratios for the target star IC 4756 12, resulting from abundance changes of C, N, or O.

Species	ΔC ±0.1 dex	ΔN ±0.1 dex	ΔO ±0.1 dex
ΔC	–	±0.01	±0.02
ΔN	∓0.10	–	±0.05
ΔO	±0.01	±0.01	–
ΔC/N	±0.19	∓0.16	∓0.01
$\Delta^{12}C/^{13}C$	±2	±2	0

and 6390.48 Å. For the analysis of the La II 5123.01 Å and 6390.48 Å lines, we applied the HFS data from (Ivans et al. 2006). We were not able to find the HFS data for the La II 6320.41 Å line, however it seems that the HFS influence is small for this line since lanthanum abundances were very similar from all three lines. Cerium abundances were determined from the Ce II lines at 5274.22, 6043.00 Å. Neodymium abundances were derived from the Nd II lines at 5092.80, 5293.20, 5319.80, 5356.97, and 5740.86 Å with the HFS adopted from Den Hartog et al. (2003). Barium and europium abundances were determined from single lines at 5853.67 and 6645.10 Å, respectively. For the Ba II line, the HFS data were taken from McWilliam (1998) and for the Eu II line from Lawler et al. (2001). The HFS was also taken into account for the determination of praseodymium abundance from Pr II lines at 5259.7 and 5322.8 Å (Sneden et al. 2009). All $\log gf$ values were calibrated to fit the solar spectrum by Kurucz (2005) with solar abundances provided by (Grevesse & Sauval 2000). Several examples of the synthetic spectra fits for some of the lines are presented in Fig. 2.

As stellar rotation ($v \sin i$) changes the shape of lines, it is also an important factor in abundance determinations from spectral syntheses. We obtained $v \sin i$ by fitting iron lines of different strengths in our investigated spectral regions.

There are two categories of uncertainties that should be considered. Firstly, there are random errors that affect each line independently and originate from the local continuum placement, from each line's fitting variations, EW measurements, or from uncertainties in atomic parameters. Uncertainties coming from the atomic data are minimized when a differential analysis is performed. Since all cluster-member stars have relatively similar parameters in our case, we can compare measurements of EWs for the same line in different stars. The mean scatter of EWs for iron lines was 4.3 mÅ. An approximate value for the random errors in the abundance determinations is given by the scatter of the derived abundances from individual lines for all elements in all stars. The mean scatter in our sample of stars is 0.06 dex.

Table 4. Effects on derived abundances, Δ[A/H], resulting from model changes for the star IC 4756 12.

Species	$\Delta T_{\rm eff}$ ±100 K	$\Delta \log g$ ±0.3	$\Delta v_{\rm t}$ ±0.3 km s^{-1}	Δ[Fe/H] ±0.1	Total
C (C_2)	0.03	0.02	0.00	0.01	0.04
N (CN)	0.10	0.03	0.01	0.01	0.11
O ([O I])	0.01	0.14	0.00	0.01	0.14
$^{12}C/^{13}C$	1	1	0	0	1.4
Na I	0.06	−0.01	0.00	0.00	0.06
Mg I	0.05	0.00	0.01	−0.01	0.05
Al I	0.06	0.00	0.01	−0.01	0.06
Si I	0.01	0.04	0.00	0.01	0.04
Ca I	0.08	−0.01	0.01	−0.01	0.08
Sc II	−0.01	0.13	0.00	0.03	0.13
Ti I	0.11	−0.01	0.00	−0.01	0.11
Ti II	−0.01	0.13	−0.01	0.03	0.13
Fe I	0.09	0.01	0.00	0.01	0.09
Fe II	−0.07	0.14	−0.01	0.04	0.15
Cr I	0.10	−0.01	−0.01	−0.01	0.10
Mn I	0.12	0.04	−0.11	0.01	0.17
Co I	0.10	0.03	0.02	0.01	0.11
Ni I	0.06	0.03	0.00	0.01	0.07
Y II	0.01	0.11	−0.25	0.04	0.27
Zr I	0.15	0.00	0.02	0.00	0.15
Ba II	0.05	0.11	−0.36	0.01	0.38
La II	0.02	0.13	−0.01	0.03	0.13
Ce II	0.01	0.13	−0.05	0.04	0.14
Pr II	0.01	0.13	−0.01	0.03	0.13
Nd II	0.03	0.14	−0.05	0.03	0.15
Eu II	−0.01	0.11	0.00	0.03	0.11

We evaluated uncertainties of atmospheric parameters using the whole sample of IC 4756 member stars. The average of slopes between [Fe/H] abundance and the excitation potential (EP) for these stars d [Fe/H]/d EP = 0.0008 ± 0.008. The error of 0.008 corresponds to the temperature change of 30 K. We can assume this as an error in our temperature estimation. The change of $\log g$ by 0.1 dex alters the Fe I and Fe II equilibrium by 0.04 dex, which is larger than our acceptable tolerance of 0.02 dex. Therefore, the error in $\log g$ determination is less than 0.1 dex. For the microturbulence velocity we minimized a slope between the Fe I abundances and the EWs. The mean d [Fe/H]/d EW = −0.0001 ± 0.0003. This error corresponds to the change of 0.05 km s^{-1}, which can be assumed as our error for the microtubulence velocity determination.

The second type of uncertainties are systematic; they are influenced by uncertainties of atmospheric parameters and affect

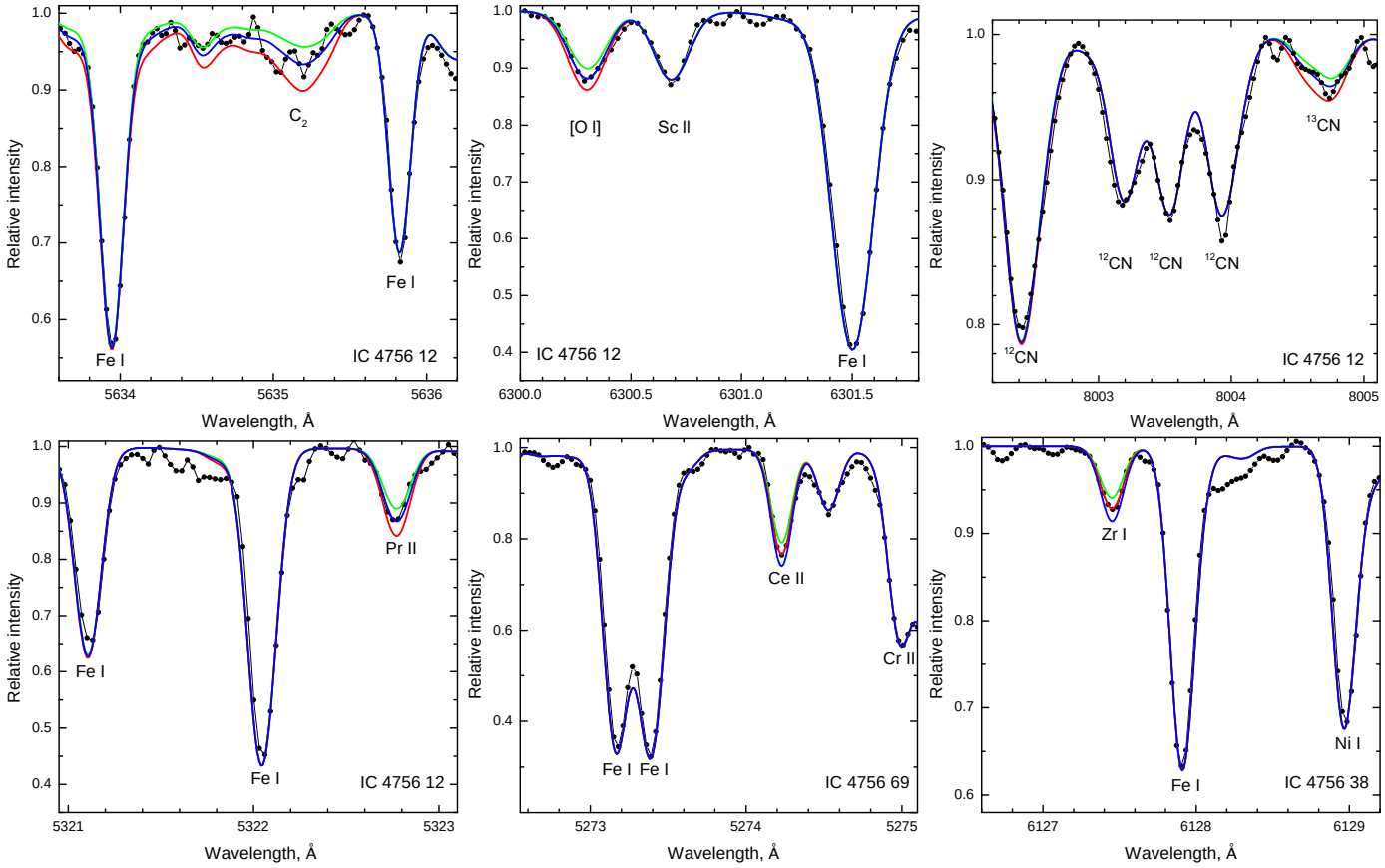

Fig. 2. Examples of the synthetic spectrum fits to various lines for the stars IC 47561 12, IC 47563 8, and IC 4756 69. The blue and green lines represent a change in abundance by ±0.1 dex to the corresponding elements, except in the case of $^{12}C/^{13}C$ where the green and red lines represent ±5.

all the lines simultaneously. Table 4 shows sensitivity of abundance estimates to changes in atmospheric parameters for the star IC 4756 12. Changes in atmospheric parameters provide relatively small abundance deviations from the initial values. The larger deviations are present for abundances derived from ionized lines, as these elements respond to the $\log g$ value changes more strongly.

Along with IC 4756 stars, we performed our atmospheric parameter and abundance determination procedures on the Arcturus's spectrum by (Hinkle et al. 2000; the results for Arcturus we present together with the IC 4756 results). Our results for Arcturus agree well with the majority of recent studies of this star (Worley et al. 2009; Ramírez & Allende Prieto 2011; Abia et al. 2012; Jofré et al. 2015).

Several examples of the synthetic spectra fits in several IC 4756 stars for some of the lines are presented in Fig. 2.

4. Results and discussion

The determined stellar atmospheric parameters and rotational velocities for our IC 4756 programme stars are presented in Table 5, and the detailed chemical abundances are in Tables 6 and 7. Mean values of element-to-iron ratios were calculated taking just definite members of IC 4756. These values with corresponding scatters are listed in Table 8 along with results from previous studies. Luck (1994) investigated one supergiant, one dwarf, and two giants. Since the investigated dwarf star was rather peculiar, we did not take its abundances while calculating the mean values presented in Table 8.

4.1. Atmospheric parameters

The average metallicity for this cluster determined in this work from nine high-probability members is close to solar – [Fe/H] = −0.02 ± 0.01. Those stars have similar atmospheric parameters and are in the red clump: the average $T_{\rm eff}$ = 5124 ± 58 K, $\log g$ = 2.72 ± 0.1, [Fe/H]= −0.02 ± 0.01, $v_{\rm t}$ = 1.38 ± 0.11 km s^{-1}.

Our mean metallicity value agrees well with the majority of the previous spectroscopic studies (Gilroy 1989, Luck 1994, Smiljanic et al. 2009, Santos et al. 2009, Ting et al. 2012), all of which provide metallicities close to solar for this cluster. Several studies by Thogersen et al. (1993) and Jacobson et al. (2007) derived a slightly sub-solar metallicity of −0.22 ± 0.12 dex and −0.15 ± 0.04 dex, respectively. These discrepant metallicities were probably caused by different line lists and/or analysis techniques.

The stars 14, 28, 44, and 52, as already discussed in Sect. 3.2, are considered as doubtful members according to the literature, however, we chose to investigate them and compare their chemical composition to other stars of the cluster. We found that stars 14, 28, and 52 have slightly lower metallicities thus we support their doubtful membership. Star 44 has the same metallicity as the cluster average, thus we leave its membership question open.

4.2. $^{12}C/^{13}C$ and C/N ratios

During a star's lifetime, complex nuclear reactions take place inside the core, producing different elements which, for the most part, stay deep inside stellar interiors. However, when the star

Table 5. Atmospheric parameters of the programme stars, the Sun, and Arcturus.

Star ID	$T_{\rm eff}$ (K)	log g	$v_{\rm t}$ (km s^{-1})	$v \sin i$ (km s^{-1})	[Fe/H]	σ Fe I	n	σ Fe II	n
				Members					
12	5135	2.6	1.45	1.6	−0.03	0.06	38	0.02	4
38	5165	2.9	1.35	1.9	0.00	0.07	38	0.05	5
42	5165	2.7	1.25	3.0	−0.01	0.04	36	0.06	5
69	5150	2.7	1.40	2.5	0.00	0.07	38	0.04	5
81	5180	2.8	1.15	3.7	−0.01	0.06	37	0.06	5
101	5135	2.8	1.40	3.2	−0.01	0.07	38	0.02	5
109	5000	2.6	1.50	2.9	−0.03	0.06	38	0.04	5
125	5150	2.8	1.45	2.6	−0.02	0.05	38	0.02	5
164	5040	2.6	1.45	2.2	−0.03	0.06	38	0.04	5
				Doubtful members					
14	4760	2.3	1.50	1.9	−0.06	0.07	37	0.04	4
28	4650	2.1	1.45	2.2	−0.10	0.08	38	0.06	5
44	5115	2.7	1.25	3.6	−0.02	0.06	37	0.07	5
52	4500	1.9	1.60	2.8	−0.12	0.08	35	0.05	5
Sun	5777	4.44	0.8	2	0.05*	0.03	38	0.01	5
Arcturus	4345	1.6	1.65	2.4	−0.58	0.04	38	0.03	5

Notes. (*) The solar iron abundance in this work is $A(\mathrm{Fe})_\odot = 7.50$ (Grevesse & Sauval 2000).

leaves the main sequence and becomes a red giant, the convective envelope of the star deepens, and the processed material from the core is brought up to the surface. By looking at abundance alterations of certain elements in stellar photospheres, we can analyse the efficiency of the transport mechanisms. Among the most sensitive elements are carbon and nitrogen. ^{12}C/^{13}C and ^{12}C/^{14}N ratios are particularly good indicators of mixing in stars.

Carbon and nitrogen abundances in evolved stars have been investigated for more than 45 yr, since studies by Day et al. (1973); Tomkin & Lambert (1974); Tomkin et al. (1975); Dearborn et al. (1976) and others. It is well known that stars undergo several mixing events during their evolution, however only one, the first dredge-up, was predicted by the classical theory of stellar evolution until a star leaves the red clump position on the HR diagram. As concerns studies of evolved stars in open clusters, inconsistencies between the ^{12}C/^{13}C ratios predicted by the classical stellar evolution model and the observational results were clearly demonstrated by Gilroy (1989). The observational results agreed relatively well with the classical model for stars in open clusters with turn-off (TO) masses larger than ~2.2 $M_\odot$. However, for stars in open clusters with lower turn-off masses the observed ^{12}C/^{13}C ratios were decreasing with decreasing TO mass.

In order to explain discrepancies between theoretical and observed abundances of mixing-sensitive chemical elements, some other transport mechanisms besides the classical convection had to be introduced. Nowadays, the most promising of these seems to be a thermohaline-induced extra-mixing. We compare our results with the first dredge-up model, a model with only the thermohaline mixing included (Charbonnel & Lagarde 2010) and with a model where rotation and thermohaline-induced mixing act together (Lagarde et al. 2012). Stellar rotation may modify an internal stellar structure even before the RGB phase, however results become visible only in later stages. The initial rotation velocity of the models on the zero age main sequence (ZAMS) was chosen at 30% of the critical velocity at that point and leads to the mean velocity of about 120 km s^{-1}

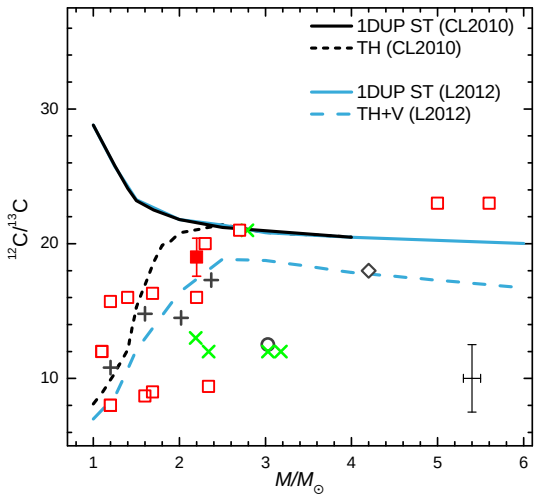

Fig. 3. Average carbon isotope ratios in clump stars of open clusters as a function of stellar TO mass. Red square indicates the value of IC 4756. Red open squares indicate results of previously investigated open clusters by Tautvaišienė et al. (2000, 2005, 2016); Mikolaitis et al. (2010, 2011a,b, 2012); Drazdauskas et al. (2016a,b). Other symbols include results from Gilroy (1989) – pluses, Luck (1994) – open circles, Smiljanic et al. (2009) – green crosses, Santrich et al. (2013) – open diamond. The solid lines (1DUP ST) represent the ^{12}C/^{13}C ratios predicted for stars at the first dredge-up with standard stellar evolutionary models of solar metallicity by Charbonnel & Lagarde (2010; black solid line) and Lagarde et al. (2012; blue solid line). The short-dashed line (TH) shows the prediction when only thermohaline extra-mixing is introduced (Charbonnel & Lagarde 2010), and the long-dashed line (TH+V) is for the model that includes both the thermohaline and rotation-induced mixing (Lagarde et al. 2012). A typical error bar is indicated (Gilroy 1989; Smiljanic et al. 2009; Charbonnel & Lagarde 2010).

(Lagarde et al. 2014). We present the comparison of our results and the models in Figs. 3 and 4. The TO mass of IC 4756 was determined using PARSEC isochrones (Bressan et al. 2012). The input metallicity of −0.02 dex was the one we determined in this

Table 6. Elemental abundances in member stars of IC 4756 and Arcturus.

El./Star	12	38	42	69	81
[C/Fe]	−0.23 ± 0.01 (02)	−0.23 ± 0.03 (02)	−0.29 ± 0.02 (02)	–	−0.29 ± 0.02 (02)
[N/Fe]	0.45 ± 0.06 (08)	0.43 ± 0.03 (08)	0.45 ± 0.04 (08)	–	0.42 ± 0.05 (07)
[O/Fe]	0.01	0.09	−0.10	–	−0.05
C/N	0.83	0.87	0.72	–	0.78
$^{12}C/^{13}C$	19	20	–	–	17
$[Na/Fe]_{LTE}$	0.23 ± 0.04 (03)	0.17 ± 0.01 (02)	0.25 ± 0.02 (03)	0.33 ± 0.04 (03)	0.19 ± 0.02 (03)
$[Na/Fe]_{NLTE}$	0.15 ± 0.07 (03)	0.06 ± 0.02 (02)	0.17 ± 0.04 (03)	0.24 ± 0.08 (03)	0.10 ± 0.06 (03)
[Mg/Fe]	0.08 ± 0.04 (02)	0.11 ± 0.01 (02)	0.15 ± 0.05 (02)	0.05 ± 0.04 (02)	−0.02 (01)
[Al/Fe]	0.10 ± 0.01 (02)	0.00 ± 0.02 (02)	0.01 ± 0.08 (02)	0.00 ± 0.07 (02)	0.03 ± 0.08 (02)
[Si/Fe]	0.00 ± 0.07 (16)	0.05 ± 0.08 (19)	0.05 ± 0.06 (19)	0.01 ± 0.06 (17)	−0.01 ± 0.05 (18)
[Ca/Fe]	0.06 ± 0.09 (06)	0.13 ± 0.08 (08)	0.11 ± 0.10 (07)	0.10 ± 0.08 (07)	0.10 ± 0.06 (08)
[Sc II/Fe]	−0.08 ± 0.05 (07)	0.03 ± 0.02 (07)	−0.06 ± 0.05 (07)	−0.02 ± 0.05 (07)	0.00 ± 0.06 (06)
[Ti I/Fe]	−0.02 ± 0.04 (13)	0.00 ± 0.04 (16)	−0.02 ± 0.04 (14)	−0.01 ± 0.04 (15)	0.01 ± 0.05 (14)
[Ti II/Fe]	−0.11 ± 0.07 (05)	−0.01 ± 0.02 (05)	−0.10 ± 0.05 (05)	−0.04 ± 0.07 (05)	−0.08 ± 0.04 (05)
[Cr/Fe]	0.08 ± 0.05 (08)	0.02 ± 0.07 (09)	0.03 ± 0.06 (09)	0.05 ± 0.08 (10)	0.01 ± 0.07 (10)
[Mn/Fe]	−0.08 ± 0.02 (03)	−0.02 ± 0.01 (03)	−0.09 ± 0.05 (03)	−0.07 ± 0.06 (03)	−0.19 ± 0.02 (03)
[Co/Fe]	−0.02 ± 0.03 (08)	−0.03 ± 0.03 (08)	−0.07 ± 0.02 (08)	−0.03 ± 0.03 (08)	−0.07 ± 0.02 (08)
[Ni/Fe]	−0.08 ± 0.09 (24)	−0.06 ± 0.07 (26)	−0.06 ± 0.10 (25)	−0.06 ± 0.08 (26)	−0.07 ± 0.07 (21)
[Y/Fe]	−0.05 ± 0.14 (05)	0.08 ± 0.09 (05)	0.02 ± 0.05 (05)	0.06 ± 0.08 (05)	−0.01 ± 0.08 (05)
[Zr/Fe]	0.20 (01)	0.24 ± 0.14 (02)	0.17 ± 0.02 (02)	0.14 ± 0.04 (02)	0.18 (01)
[Ba/Fe]	0.20 (01)	0.23 (1)	0.24 (1)	0.30 (01)	0.22 (01)
[La/Fe]	0.20 ± 0.02 (03)	0.23 ± 0.05 (03)	0.14 ± 0.02 (03)	0.19 ± 0.03 (02)	0.23 ± 0.04 (03)
[Ce/Fe]	0.21 ± 0.10 (02)	0.27 ± 0.11 (02)	0.18 ± 0.07 (02)	0.17 ± 0.06 (02)	0.18 ± 0.04 (02)
[Pr/Fe]	0.21 ± 0.03 (02)	0.18 ± 0.07 (02)	0.10 ± 0.01 (02)	0.14 ± 0.06 (02)	0.16 ± 0.02 (02)
[Nd/Fe]	0.08 ± 0.06 (05)	0.14 ± 0.06 (05)	0.03 ± 0.06 (05)	0.13 ± 0.04 (05)	0.11 ± 0.07 (05)
[Eu/Fe]	0.02 (01)	0.11 (01)	0.03 (01)	0.04 (01)	0.03 (01)
El./Star	101	109	125	164	Arcturus
[C/Fe]	−0.23 ± 0.03 (02)	−0.24 ± 0.05 (02)	−0.26 (01)	−0.28 ± 0.02 (02)	0.03 ± 0.01 (02)
[N/Fe]	0.46 ± 0.04 (07)	0.47 ± 0.03 (08)	0.46 ± 0.05 (08)	0.45 ± 0.03 (08)	0.29 ± 0.02 (08)
[O/Fe]	0.05	0.02	0.02	0.02	0.55
C/N	0.81	0.78	0.76	0.74	2.19
$^{12}C/^{13}C$	–	–	17	20	7
$[Na/Fe]_{LTE}$	0.19 ± 0.06 (03)	0.24 ± 0.04 (03)	0.19 ± 0.04 (03)	0.22 ± 0.02 (03)	0.20 ± 0.05 (03)
$[Na/Fe]_{NLTE}$	0.11 ± 0.11 (03)	0.16 ± 0.09 (03)	0.11 ± 0.01 (03)	0.14 ± 0.03 (03)	0.16 ± 0.06 (03)
[Mg/Fe]	0.03 ± 0.05 (02)	0.04 ± 0.02 (02)	0.11 ± 0.01 (02)	0.14 ± 0.02 (02)	0.43 ± 0.01 (02)
[Al/Fe]	0.01 ± 0.05 (02)	0.05 ± 0.04 (02)	0.07 ± 0.04 (02)	0.06 ± 0.01 (02)	0.43 ± 0.07 (03)
[Si/Fe]	0.06 ± 0.07 (18)	0.08 ± 0.08 (17)	0.06 ± 0.06 (18)	0.07 ± 0.07 (17)	0.25 ± 0.04 (18)
[Ca/Fe]	0.09 ± 0.06 (07)	0.16 ± 0.09 (07)	0.12 ± 0.08 (07)	0.12 ± 0.06 (08)	0.18 ± 0.06 (08)
[Sc II/Fe]	0.01 ± 0.06 (06)	0.01 ± 0.07 (07)	0.03 ± 0.07 (07)	0.01 ± 0.06 (07)	0.15 ± 0.04 (07)
[Ti I/Fe]	−0.04 ± 0.04 (13)	0.01 ± 0.05 (12)	0.02 ± 0.05 (15)	0.01 ± 0.04 (13)	0.27 ± 0.05 (16)
[Ti II/Fe]	0.02 ± 0.06 (05)	0 ± 0.05 (05)	−0.02 ± 0.02 (05)	−0.04 ± 0.04 (05)	0.23 ± 0.05 (04)
[Cr/Fe]	−0.01 ± 0.04 (09)	0.00 ± 0.07 (09)	0.01 ± 0.06 (10)	0.04 ± 0.06 (09)	−0.03 ± 0.07 (10)
[Mn/Fe]	−0.06 ± 0.05 (03)	−0.07 ± 0.06 (03)	−0.02 ± 0.03 (03)	−0.04 ± 0.07 (03)	−0.18 ± 0.08 (03)
[Co/Fe]	−0.06 ± 0.03 (08)	−0.01 ± 0.03 (08)	−0.02 ± 0.02 (08)	−0.04 ± 0.04 (08)	0.2 ± 0.03 (08)
[Ni/Fe]	−0.05 ± 0.07 (25)	−0.05 ± 0.08 (24)	−0.04 ± 0.05 (24)	−0.03 ± 0.05 (26)	0.02 ± 0.09 (24)
[Y/Fe]	0.06 ± 0.10 (05)	0.03 ± 0.10 (05)	0.09 ± 0.06 (05)	0.02 ± 0.12 (05)	−0.08 ± 0.16 (05)
[Zr/Fe]	0.11 ± 0.10 (02)	0.22 ± 0.08 (02)	0.21 ± 0.07 (02)	0.19 ± 0.04 (02)	−0.02 ± 0.11 (02)
[Ba/Fe]	0.25 (01)	0.18 ± 0 (1)	0.23 (01)	0.18 (01)	−0.22 (01)
[La/Fe]	0.27 ± 0.03 (03)	0.24 ± 0.03 (03)	0.26 ± 0.01 (02)	0.24 ± 0.01 (03)	0.07 ± 0.05 (03)
[Ce/Fe]	0.21 ± 0.06 (02)	0.24 ± 0.11 (02)	0.24 ± 0.08 (02)	0.21 ± 0.07 (02)	−0.10 ± 0.11 (02)
[Pr/Fe]	0.19 ± 0.03 (02)	0.22 ± 0.06 (02)	0.22 ± 0.04 (02)	0.19 ± 0.01 (02)	0.19 ± 0.04 (02)
[Nd/Fe]	0.16 ± 0.07 (05)	0.16 ± 0.03 (05)	0.15 ± 0.06 (05)	0.13 ± 0.05 (05)	−0.08 ± 0.04 (05)
[Eu/Fe]	0.10 (01)	0.08 (01)	0.13 (01)	0.14 (01)	0.38 (01)

Notes. The elemental abundance ratios are presented together with the abundance scatter from individual lines and a number of lines used for the analysis.

Table 7. Elemental abundances in doubtful member stars of IC 4756.

El./Star	14	28	44	52
[C/Fe]	−0.24 ± 0.03 (02)	−0.20 (01)	−0.32 ± 0.02 (02)	−0.18 ± 0.03 (02)
[N/Fe]	0.50 ± 0.03 (08)	0.37 ± 0.02 (08)	0.42 ± 0.04 (08)	0.49 ± 0.05 (08)
[O/Fe]	0.10	0.09	−0.08	0.14
C/N	0.72	–	0.72	0.85
$^{12}C/^{13}C$	19	–	–	–
$[Na/Fe]_{LTE}$	0.31 ± 0.03 (03)	0.24 ± 0.06 (03)	0.19 ± 0.01 (03)	0.28 ± 0.06 (03)
$[Na/Fe]_{NLTE}$	0.23 ± 0.07 (03)	0.16 ± 0.03 (03)	0.10 ± 0.05 (03)	0.20 ± 0.04 (03)
[Mg/Fe]	0.13 ± 0.03 (02)	0.14 ± 0.01 (02)	0.03 ± 0.06 (02)	0.12 ± 0.02 (02)
[Al/Fe]	0.09 ± 0.04 (02)	0.14 ± 0.04 (02)	0.06 ± 0.05 (02)	0.19 ± 0.07 (02)
[Si/Fe]	0.13 ± 0.1 (17)	0.16 ± 0.10 (17)	0.03 ± 0.08 (16)	0.18 ± 0.10 (13)
[Ca/Fe]	0.14 ± 0.10 (07)	0.08 ± 0.09 (05)	0.12 ± 0.06 (07)	0.17 ± 0.11 (08)
[Sc II/Fe]	0.08 ± 0.04 (06)	0.02 ± 0.09 (06)	0.01 ± 0.03 (05)	0.04 ± 0.10 (06)
[Ti I/Fe]	0.02 ± 0.05 (16)	0.02 ± 0.07 (17)	0.01 ± 0.06 (15)	0.00 ± 0.08 (18)
[Ti II/Fe]	0.03 ± 0.02 (05)	−0.02 ± 0.02 (05)	−0.06 ± 0.05 (05)	0.07 ± 0.03 (05)
[Cr/Fe]	0.02 ± 0.08 (10)	0.03 ± 0.07 (09)	0.07 ± 0.10 (10)	0.02 ± 0.07 (09)
[Mn/Fe]	−0.12 ± 0.05 (03)	−0.07 ± 0.08 (03)	−0.16 ± 0.02 (03)	−0.07 ± 0.08 (03)
[Co/Fe]	−0.01 ± 0.02 (08)	−0.02 ± 0.04 (08)	−0.07 ± 0.04 (08)	0.02 ± 0.04 (08)
[Ni/Fe]	0.00 ± 0.11 (21)	−0.02 ± 0.11 (24)	−0.07 ± 0.07 (26)	0.03 ± 0.12 (24)
[Y/Fe]	0.01 ± 0.10 (05)	0.05 ± 0.12 (05)	0.01 ± 0.07 (05)	0.05 ± 0.15 (05)
[Zr/Fe]	0.21 ± 0.06 (02)	0.15 ± 0.01 (02)	0.16 ± 0.09 (02)	0.13 ± 0.02 (02)
[Ba/Fe]	0.15 (01)	0.19 (01)	0.27 (01)	0.19 (01)
[La/Fe]	0.30 ± 0.06 (03)	0.23 ± 0.05 (03)	0.20 ± 0.07 (03)	0.30 ± 0.06 (03)
[Ce/Fe]	0.24 ± 0.14 (02)	0.21 ± 0.13 (02)	0.20 ± 0.15 (02)	0.29 ± 0.12 (02)
[Pr/Fe]	0.27 ± 0.04 (02)	0.22 ± 0.01 (02)	0.14 ± 0.03 (02)	0.31 ± 0.06 (02)
[Nd/Fe]	0.10 ± 0.04 (05)	0.09 ± 0.04 (05)	0.04 ± 0.05 (05)	0.15 ± 0.08 (05)
[Eu/Fe]	0.15 (01)	0.14 (01)	0.04 (01)	0.17 (01)

Notes. The elemental abundance ratios are presented together with the abundance scatter from individual lines and a number of lines used for the analysis.

work, and we took the cluster age of 0.89 Gyr as determined by Strassmeier et al. (2015). We consider all the stars in our analysis as being in a He-core burning stage. Our determined TO mass of IC 4756 is around 2.2 $M_{\odot}$.

The average $^{12}C/^{13}C$ value as obtained from three evolved IC 4756 giants is 19 ± 1.4 and the mean C/N ratio is equal to 0.79 ± 0.05. The previous analysis of C/N ratios were made by Luck (1994) and Smiljanic et al. (2009). Our result agrees well with the one by Luck (1994) however the mean C/N value reported by Smiljanic et al. (2009) is slightly larger and has a larger scatter (see Table 8). From the same stars, Smiljanic et al. (2009) obtained a somewhat lower result for $^{12}C/^{13}C$ and a larger scatter. The Luck (1994) result lies in the middle with a result from only one star with the value of 15. The mean $^{12}C/^{13}C$ ratio determined for this cluster by Gilroy (1989) agrees well with our determination.

From the comparison of our result and the theoretical models we can see that the mean values of $^{12}C/^{13}C$ and C/N ratios lie between the model with only the thermohaline extra-mixing included and the model which also includes the rotation-induced mixing. The rotation was most probably smaller in the investigated IC 4756 stars than 120 km s^{-1} when they were on the ZAMS. When looking at the C/N values from ours and previous studies, it is obvious that the pure thermohaline extra-mixing model is preferred for the open clusters with the TO masses below 2.2 $M_{\odot}$. There were some debates (see Wachlin et al. 2014 and references therein) that thermohaline convection models greatly overestimate the effects of such mixing, and some other explanation might be needed.

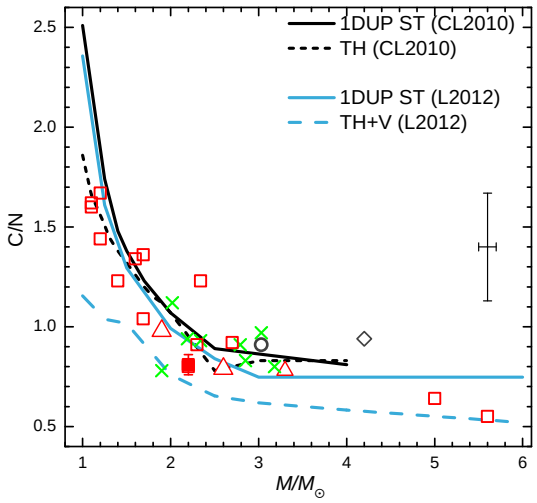

Fig. 4. Average carbon-to-nitrogen ratios in clump stars of open clusters as a function of stellar TO mass. In addition to symbols in Fig. 3, here we include the results from Tautvaišienė et al. (2015) as red open triangles.

4.3. Sodium

Sodium, besides carbon and nitrogen, is one of the other mixing-sensitive chemical elements. Theoretical models by Lagarde et al. (2012) predict a significant increase of sodium abundance after the first dredge-up for stars with turn-off masses of around 2 $M_{\odot}$, and an even larger overabundance if the

Table 8. Comparison of mean IC 4756 abundances determined in this work and previous studies.

Element /Resolution	This study 48 000	Luck (1994) 18 000	Jacobson et al. (2007) 15 000	Smiljanic et al. (2009) 48 000	Pace et al. (2010) 100 000	Maiorca et al. (2011) 100 000	Ting et al. (2012) 30 000
[C/Fe]	**−0.26 ± 0.03**	−0.27 ± 0.05	...	**−0.15 ± 0.02**	...	...	...
[N/Fe]	**0.45 ± 0.02**	0.54 ± 0.16	...	**0.43 ± 0.07**	...	...	...
[O/Fe]	**0.01 ± 0.05**	−0.17 ± 0.09	...	**−0.01 ± 0.01**	<0.07	...	...
C/N	**0.79 ± 0.05**	0.80 ± 0.20	...	**1.05 ± 0.12**	...	...	...
$^{12}C/^{13}C$	**19 ± 1.4**	**15**	...	**13 ± 3.1**	...	...	...
$[Na/Fe]_{LTE}$	0.22 ± 0.05	0.14 ± 0.01	0.57 ± 0.06	...	0.11 ± 0.04	...	0.21 ± 0.15
$[Na/Fe]_{NLTE}$	0.14 ± 0.05	...	...	−0.01 ± 0.04	...	...	...
[Mg/Fe]	0.08 ± 0.05	0.20 ± 0.14	...	−0.05 ± 0.02	...	...	0.12 ± 0.13
[Al/Fe]	0.04 ± 0.03	0.07 ± 0.21	0.29 ± 0.08	...	−0.11 ± 0.05	...	0.12 ± 0.12
[Si/Fe]	0.04 ± 0.03	0.23 ± 0.04	0.34 ± 0.06	0.06 ± 0.04	0.02 ± 0.01	...	0.13 ± 0.13
[Ca/Fe]	0.11 ± 0.03	−0.07 ± 0.13	0.07 ± 0.08	0.02 ± 0.04	−0.02 ± 0.03	...	0.05 ± 0.16
[Sc II/Fe]	−0.01 ± 0.04	0.03 ± 0.12	...	0.06 ± 0.07	...	...	...
[Ti I/Fe]	0.00 ± 0.02	−0.09 ± 0.13	...	−0.04 ± 0.01	0.03 ± 0.03	...	...
[Ti II/Fe]	−0.03 ± 0.05	...	...	...	...	...	0.28 ± 0.08
[Fe I/H]	−0.02 ± 0.01	−0.05 ± 0.05	−0.15 ± 0.04	0.04 ± 0.03	0.08 ± 0.02	0.01 ± 0.03	−0.01 ± 0.10
[Fe II/H]	−0.02 ± 0.02	−0.04 ± 0.04	...	0.04 ± 0.03	...	...	0.00 ± 0.11
[Cr/Fe]	0.03 ± 0.03	0.08 ± 0.04	...	0.04 ± 0.05	0.00 ± 0.03	...	0.03 ± 0.15
[Mn/Fe]	**−0.07 ± 0.05**	0.20 ± 0.18	...	...	...	...	...
[Co/Fe]	**−0.04 ± 0.02**	0.32 ± 0.16	...	0.06 ± 0.04	...	...	...
[Ni/Fe]	−0.06 ± 0.01	0.08 ± 0.07	0.08 ± 0.05	−0.01 ± 0.02	−0.04 ± 0.01	...	0.03 ± 0.13
[Y/Fe]	**0.03 ± 0.04**	0.37 ± 0.03	...	...	...	0.11 ± 0.01	...
[Zr/Fe]	**0.18 ± 0.04**	0.25 ± 0.13	...	...	...	0.09 ± 0.02	...
[Ba/Fe]	**0.23 ± 0.04**	0.01 ± 0.21	...	...	...	...	**0.00 ± 0.14**
[La/Fe]	**0.22 ± 0.04**	...	...	...	...	0.19 ± 0.01	...
[Ce/Fe]	**0.21 ± 0.03**	...	...	...	...	0.16 ± 0.02	...
[Pr/Fe]	**0.18 ± 0.04**	...	...	...	...	...	...
[Nd/Fe]	**0.12 ± 0.04**	0.37 ± 0.01	...	...	...	...	...
[Eu/Fe]	**0.08 ± 0.04**	0.16	...	...	...	...	...

Notes. The abundances marked in bold were determined using spectral syntheses. The remaining abundances were derived from EWs. Along with the mean elemental abundances, values of root mean square between stars are presented.

extra-mixing is taken into account. Our results and several other recent NLTE determinations of sodium abundances in other studies (Drazdauskas et al. 2016b; MacLean et al. 2015; Smiljanic et al. 2016) are displayed in Fig. 5 together with the theoretical models by Lagarde et al. (2012). Following Smiljanic et al. (2016), only high-probability giant stars were extracted from the paper by MacLean et al. (2015). The theoretical models show how sodium abundance increases in relation to the TO mass. At the TO mass of IC 4756, which is around 2.2 $M_{\odot}$, the average NLTE sodium abundance, as in case of $^{12}C/^{13}C$ and C/N, lies between the theoretical model which includes the thermohaline- and rotation-induced extra-mixing and the model of the first dredge-up (or the model of pure thermohaline mixing since they both give very close [Na/Fe] values). These results confirm a conclusion by other investigators who suggest that the trend of sodium abundance increases in relation to a TO mass and is most probably caused by internal stellar evolutionary processes (Smiljanic et al. 2016 and references therein).

4.4. α-Elements

α-Elements are of particular interest when studying Galactic archaeology due to a different timescale of their production compared to iron-peak elements. These elements are mainly produced in massive stars, thus any visible enhancement in their abundances can reveal differences of star formation histories in different parts of the Galaxy.

Figure 6 displays the determined average α-element abundance in IC 4756 together with results from other studies. The average abundances were calculated simply by taking the average of [Mg/Fe], [Ca/Fe], [Si/Fe], and [Ti/Fe] values. We find no α-element enhancement in our cluster, and our result shows an almost perfect match with the theoretical model by Pagel & Tautvaisiene (1997).

We take a look at oxygen and magnesium abundances separately in Fig. 7 and compare them with models by Magrini et al. (2009) and abundance results from other studies. Oxygen is one of the more difficult elements to precisely analyse due to the relations with carbon and nitrogen. Therefore, for the comparison we take the results from studies where the oxygen abundance was determined in the same way as in this study (Mikolaitis et al. 2010, 2011a,b; Tautvaišienė et al. 2015; Drazdauskas et al. 2016a,b). For the magnesium, we have taken results from the same authors as other α-elements (Jacobson et al. 2008, 2009; Friel et al. 2010; Mikolaitis et al. 2010, 2011a,b; Reddy et al. 2012, 2013, 2015; Mishenina et al. 2015). The models depict the oxygen and magnesium abundance trends in relation to the Galactocentric distance. Our results for IC 4756 follow the models, and at R_{gc} of 8.1 kpc show no visible over- or under-abundances for oxygen or magnesium.

4.5. Iron-peak elements

The mean abundances of five iron-peak elements investigated in our sample of IC 4756 RGB stars display no significant deviations from the mean iron abundance. These results are consistent with previous abundance determinations for this cluster (see

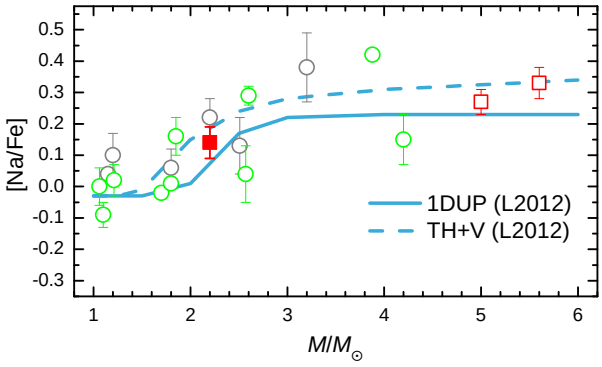

Fig. 5. Mean $[Na/Fe]_{NLTE}$ abundances in open clusters compared to theoretical models by Lagarde et al. (2012). The result obtained in this study is marked with the red square. The red open squares indicate results from Drazdauskas et al. (2016b). The results from MacLean et al. (2015) are indicated as the open grey circles and from Smiljanic et al. (2016) are shown as the green open circles.

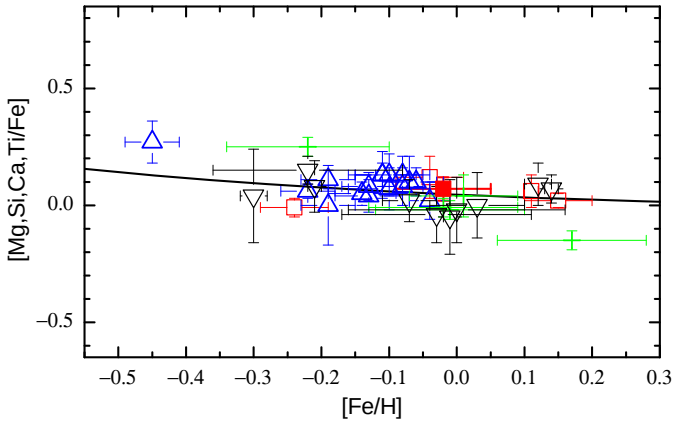

Fig. 6. Mean α-element abundances in open cluster RGB stars. The result for this study is indicated by the red circle. Results from Tautvaišienė et al. (2005); Mikolaitis et al. (2010, 2011a,b); Drazdauskas et al. (2016b) are marked as the red open squares. The blue triangles indicate results from Reddy et al. (2012, 2013, 2015); the green plus signs from Mishenina et al. (2015); and the black reverse triangles from Friel et al. (2010); Jacobson et al. (2008, 2009). The black line represents the Galactic disc evolution model by Pagel & Tautvaisiene (1995).

Table 8). Larger discrepancies are coming from the study by Luck (1994) who reported relatively large values and scatters for manganese and cobalt, which might be caused by uncertainties in accounting for a hyperfine structure in these element lines.

4.6. Neutron-capture elements

Along with our results, in Table 8 we present abundances of neutron-capture elements determined in IC 4756 by several other studies. The results by Luck (1994) were averaged from one supergiant and two giants. Maiorca et al. (2011) investigated three dwarfs using an EW method, while Ting et al. (2012) from 12 giant stars (10 of which are common with our work) determined solely the barium abundance.

Y and Zr could be attributed to the elements that lie in the first *s*-process peak and are referred to as the light *s*-process elements. Their production scenarios are similar. In the Sun, 74% of yttrium and 67% of zirconium are produced via the *s*-process (Travaglio et al. 2004). The main *s*-process component, which gathers free neutrons from low-mass AGB stars, contributes to

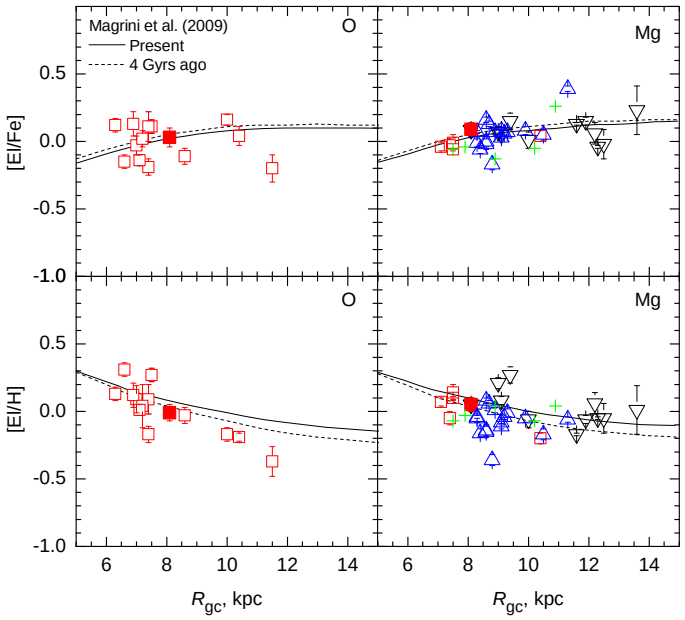

Fig. 7. Mean oxygen and magnesium abundances compared to the theoretical models by Magrini et al. (2009). The oxygen results are taken from Tautvaišienė et al. (2005, 2015); Mikolaitis et al. (2010, 2011a,b); Drazdauskas et al. (2016a,b). Symbols are the same as in Fig. 6.

69% of Y and to 65% of Zr, while the weak *s*-process component contributes only 5% of Y and 2% of Zr. The rapid neutron capture process (*r*-process) is responsible for 8% of Y and 15% of Zr. A responsible process for production of the remaining 18% of Y and Zr is debatable. Travaglio et al. (2004) called this process the lighter element primary process (LEPP) which possibly acts in low-metallicity massive stars. Therefore, due to the similarities of production of Y and Zr, abundances of these elements should be similar. As displayed in Fig. 8, the clusters' results from various studies of Y and Zr exhibit abundances roughly confined between 0 and 0.2 dex, with several values scattered around this range. Our programme cluster IC 4756 displays average abundance ratios of 0.03 dex for [Y/Fe], and 0.18 dex for [Zr/Fe]. Abundances of those elements are not similar, however, they follow the modeled trends by Maiorca et al. (2012) quite well.

Ba, La, and Ce belong to the second s-process peak. According to Arlandini et al. (1999), *s*-process contributes to Ba, La, and Ce production by 81%, 62%, and 77%, respectively. The newer study by Bisterzo et al. (2016) provided slightly different results, indicating the *s*-process enrichment of Ba, La, and Ce by 83%, 73%, and 81%, respectively. This strengthens a key feature of the elements in the second peak that all elements beyond $A = 90$, except for Pb, are mainly produced via the main *s*-process component (Käppeler et al. 2011). The remaining abundances of these elements are provided by the *r*-process. Thus, the similarity of the Ba, La, and Ce production should be reflected in their abundance similarities. By looking at Table 8, we see that the average abundances of these elements are identical in our work.

Nd and Pr are elements that have a mixed origin, as they are produced via *s*- and *r*-processes in roughly equal fractions. As reported by Arlandini et al. (1999) and Bisterzo et al. (2016), *s*-process produces around 49% of Pr and 56% of Nd, while the remaining fractions of the elements are created via the *r*-process −51% and 44%, respectively. Rather similar abundances of Nd and Pr in IC 4756 confirm their formation scenario.

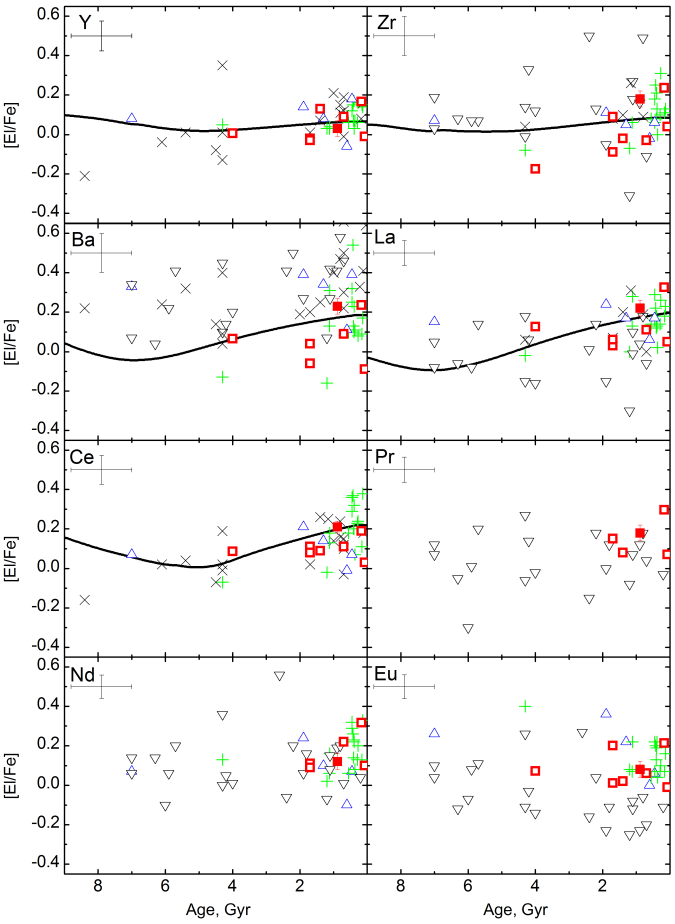

Fig. 8. Averaged values of neutron-capture element abundances vs. age in IC 4756 (red filled squares) and other previously investigated clusters. The green plus signs indicate results by Reddy et al. (2012, 2013, 2015); the blue triangles – results by Mishenina et al. (2015); the black crosses – results by D'Orazi et al. (2009) and Maiorca et al. (2011); the black reverse triangles – results by Jacobson & Friel (2013) and Overbeek et al. (2016); the empty red squares – results from our previous studies by Tautvaišienė et al. (2000, 2005), Mikolaitis et al. (2010, 2011a,b) and Drazdauskas et al. (2016a). The adopted approximate age errors of 0.9 Gyr are based on determinations by (Salaris et al. 2004). The continuous lines indicate a chemical evolution model by Maiorca et al. (2012) at the Solar radius.

Finally, europium is an almost purely *r*-process-dominated element, as only 6% of its production takes place via the *s*-process and the remaining 94% via the *r*-process (Bisterzo et al. 2016). The europium abundance in IC 4756 is similar to the thin disc chemical content (e.g. Pagel & Tautvaisiene 1997).

From the comparison of n-capture chemical element abundances in open clusters and a semi-empirical models of the Galactic thin disc chemical evolution by Pagel & Tautvaisiene (1997), we see that *s*-process-dominated elements, and especially barium, have higher abundances for many open clusters. This phenomenon can be explained by the young age of these clusters and a larger contribution of low-mass asymptotic giant branch stars in producing *s*-process elements at the time these clusters were formed (c.f. D'Orazi et al. 2009, Maiorca et al. 2011). At the same time, the *r*-process-dominated element europium results agree well with the thin disc model.

In Fig. 8 we can see how abundances of n-capture element abundances in open clusters depend on cluster ages. IC 4756 is a relatively young open cluster with an age of around 0.8 Gyr. Abundances of all investigated elements in IC 4756 agree well with the model by Maiorca et al. (2012) for the Solar radius. This is applicable also to barium (nine IC 4756 giants provide the average [Ba/Fe] = 0.22 ± 0.03), while [Ba/Fe] in OC investigated in several other studies at similar ages have values from 0.3 dex to 0.6 dex exceeding predictions of the model (see Fig. 8).

5. Conclusions

Recognising the role that open clusters play in the establishment of Galactic chemical evolution models, we performed a detailed high-resolution spectroscopic analysis of the open cluster IC 4756. We determined the main atmospheric parameters of 13 giant stars, with 9 of them being the high-probability members of the cluster. We also carried out a comprehensive analysis of 23 chemical elements made in various stellar phases and processes. The key results of our analysis are as follows:

- IC 4756 has a metallicity close to Solar. [Fe/H] = −0.02 ± 0.01, whereas other iron-peak elements do not differ by more than 0.1 dex from Solar values.
- Our determined average α-element abundances show a slight enrichment of 0.07 dex compared to iron, however that is expected from the thin disc chemical evolution model by Pagel & Tautvaisiene (1995). The results for oxygen and magnesium show no deviation from the models by Magrini et al. (2009), also at the given galactocentric distance of 8.1 kpc.
- The mean ratio of carbon and nitrogen, C/N = 0.79 ± 0.05, and the carbon isotope ratio, $^{12}C/^{13}C$ = 19 ± 1.41, are altered more than predicted in the first dredge-up model, and lie between the model where only the thermohaline extra-mixing is included and the model which also includes the rotation-induced mixing (Lagarde et al. 2012). The value we obtained for sodium with NLTE corrections, [Na/Fe] = 0.14 ± 0.05, is larger than the first dredge-up prediction, however this is lower than the value predicted by the model of thermohaline- and rotation-induced extra mixing. The rotation was most probably smaller in IC 4756 stars than the 30% of the critical rotation velocity at the ZAMS.
- Being relatively young, the open cluster IC 4756 displays a moderate enrichment of *s*-process-dominated chemical elements compared to the Galactic thin disc model (Pagel & Tautvaisiene 1997) and confirms the enrichment of *s*-process-dominated elements in young open clusters compared to the older ones. Abundances of all investigated *s*-process-dominated elements in IC 4756 agree well with the model for the Solar radius by Maiorca et al. (2012). The *r*-process-dominated element europium abundance agrees with the thin disc abundance.

Acknowledgements. This research has made use of the WEBDA database (operated at the Department of Theoretical Physics and Astrophysics of the Masaryk University, Brno), of SIMBAD (operated at CDS, Strasbourg), of VALD (Kupka et al. 2000), and of NASA's Astrophysics Data System. Bertrand Plez (University of Montpellier II) and Guillermo Gonzalez (Washington State University) were particularly generous in providing us with atomic data for CN and C_2, respectively. We thank Laura Magrini for sharing with us the Galactic chemical evolution models. We also thank the referee for helpful suggestions and comments that improved the quality of this paper. VB, AD, GT, YC were partially supported by the grant from the Research Council of Lithuania (MIP-082/2015). RS acknowledges support by the National Science Center of Poland through the grant 2012/07/B/ST9/04428.

References

Abia, C., Palmerini, S., Busso, M., & Cristallo, S. 2012, A&A, 548, A55
Alcaino, G. 1965, Lowell Observatory Bulletin, 6, 167
Angelou, G. C., Stancliffe, R. J., Church, R. P., Lattanzio, J. C., & Smith, G. H. 2012, ApJ, 749, 128
Arlandini, C., Käppeler, F., Wisshak, K., et al. 1999, ApJ, 525, 886
Baumgardt, H., Dettbarn, C., & Wielen, R. 2000, A&AS, 146, 251
Bisterzo, S., Travaglio, C., Wiescher, M., et al. 2016, J. Phys. Conf. Ser., 665, 012023
Bressan, A., Marigo, P., Girardi, L., et al. 2012, MNRAS, 427, 127
Cantiello, M., & Langer, N. 2010, A&A, 521, A9
Cardon, B. L., Smith, P. L., Scalo, J. M., Testerman, L., & Whaling, W. 1982, ApJ, 260, 395
Casamiquela, L., Carrera, R., Jordi, C., et al. 2016, MNRAS, 458, 3150
Chanamé, J., Pinsonneault, M., & Terndrup, D. M. 2005, ApJ, 631, 540
Charbonnel, C. 2006, in EAS Pub. Ser., 19, 125
Charbonnel, C., & Lagarde, N. 2010, A&A, 522, A10
Day, R. W., Lambert, D. L., & Sneden, C. 1973, ApJ, 185, 213
De Silva, G. M., Freeman, K. C., Bland-Hawthorn, J., et al. 2015, MNRAS, 449, 2604
Dearborn, D. S. P., Eggleton, P. P., & Schramm, D. N. 1976, ApJ, 203, 455
Den Hartog, E. A., Lawler, J. E., Sneden, C., & Cowan, J. J. 2003, ApJS, 148, 543
Den Hartog, E. A., Lawler, J. E., Sobeck, J. S., Sneden, C., & Cowan, J. J. 2011, ApJS, 194, 35
Denissenkov, P. A. 2010, ApJ, 723, 563
Dias, W. S., Monteiro, H., Caetano, T. C., et al. 2014, A&A, 564, A79
D'Orazi, V., Magrini, L., Randich, S., et al. 2009, ApJ, 693, L31
D'Orazi, V., Biazzo, K., Desidera, S., et al. 2012, MNRAS, 423, 2789
D'Orazi, V., De Silva, G. M., & Melo, C. F. H. 2017, A&A, 598, A86
Drazdauskas, A., Tautvaišienė, G., Randich, S., et al. 2016a, A&A, 589, A50
Drazdauskas, A., Tautvaišienė, G., Smiljanic, R., Bagdonas, V., & Chorniy, Y. 2016b, MNRAS, 462, 794
Friel, E. D., Jacobson, H. R., & Pilachowski, C. A. 2010, AJ, 139, 1942
Frinchaboy, P. M., & Majewski, S. R. 2008, AJ, 136, 118
Gaia Collaboration (Prusti, T., et al.) 2016, A&A, 595, A1
Gilmore, G., Randich, S., Asplund, M., et al. 2012, The Messenger, 147, 25
Gilroy, K. K. 1989, ApJ, 347, 835
Gonzalez, G., Lambert, D. L., Wallerstein, G., et al. 1998, ApJS, 114, 133
Grevesse, N., & Sauval, A. J. 2000, in Origin of Elements in the Solar System, Implications of Post-1957 Observations, ed. O. Manuel, 261
Gurtovenko, E. A., & Kostyk, R. I. 1989, Fraunhofers Spectrum and a System of Solar Oscillator Strengths (Kiev: Nauk. dumka), 200
Gustafsson, B., Edvardsson, B., Eriksson, K., et al. 2008, A&A, 486, 951
Hekker, S., & Meléndez, J. 2007, A&A, 475, 1003
Herzog, A. D., Sanders, W. L., & Seggewiss, W. 1975, A&AS, 19, 211
Hinkle, K., Wallace, L., Valenti, J., & Harmer, D. 2000, Visible and Near Infrared Atlas of the Arcturus Spectrum 3727–9300 Å (San Francisco: ASP)
Iben, Jr. I. 1965, ApJ, 142, 1447
Ivans, I. I., Simmerer, J., Sneden, C., et al. 2006, ApJ, 645, 613
Jacobson, H. R., & Friel, E. D. 2013, AJ, 145, 107
Jacobson, H. R., Friel, E. D., & Pilachowski, C. A. 2007, AJ, 134, 1216
Jacobson, H. R., Friel, E. D., & Pilachowski, C. A. 2008, AJ, 135, 2341
Jacobson, H. R., Friel, E. D., & Pilachowski, C. A. 2009, AJ, 137, 4753
Jofré, P., Heiter, U., Soubiran, C., et al. 2015, A&A, 582, A81
Johansson, S., Litzén, U., Lundberg, H., & Zhang, Z. 2003, ApJ, 584, L107
Käppeler, F., Gallino, R., Bisterzo, S., & Aoki, W. 2011, Rev. Mod. Phys., 83, 157
Kaufer, A., Stahl, O., Tubbesing, S., et al. 1999, The Messenger, 95, 8
Kopff, E. 1943, Astron. Nachr., 274, 69
Kunder, A., Kordopatis, G., Steinmetz, M., et al. 2017, AJ, 153, 75
Kupka, F. G., Ryabchikova, T. A., Piskunov, N. E., Stempels, H. C., & Weiss, W. W. 2000, Baltic Astron., 9, 590
Kurucz, R. L. 2005, Mem. Soc. Astron. It. Supp., 8, 189
Lagarde, N., Charbonnel, C., Decressin, T., & Hagelberg, J. 2011, A&A, 536, A28
Lagarde, N., Decressin, T., Charbonnel, C., et al. 2012, A&A, 543, A108
Lagarde, N., Anderson, R. I., Charbonnel, C., et al. 2014, A&A, 570, C2
Lattanzio, J. C., Siess, L., Church, R. P., et al. 2015, MNRAS, 446, 2673
Lawler, J. E., Wickliffe, M. E., den Hartog, E. A., & Sneden, C. 2001, ApJ, 563, 1075
Lind, K., Asplund, M., Barklem, P. S., & Belyaev, A. K. 2011, A&A, 528, A103
Luck, R. E. 1994, ApJS, 91, 309
MacLean, B. T., De Silva, G. M., & Lattanzio, J. 2015, MNRAS, 446, 3556
Magrini, L., Sestito, P., Randich, S., & Galli, D. 2009, A&A, 494, 95
Maiorca, E., Randich, S., Busso, M., Magrini, L., & Palmerini, S. 2011, ApJ, 736, 120
Maiorca, E., Magrini, L., Busso, M., et al. 2012, ApJ, 747, 53
Masseron, T., & Gilmore, G. 2015, MNRAS, 453, 1855
Matteucci, F. 1992, Mem. Soc. Astron. It., 63, 301
Matteucci, F., & Greggio, L. 1986, A&A, 154, 279
McWilliam, A. 1998, AJ, 115, 1640
Mermilliod, J.-C., Andersen, J., Latham, D. W., & Mayor, M. 2007, A&A, 473, 829
Mermilliod, J. C., Mayor, M., & Udry, S. 2008, A&A, 485, 303
Mikolaitis, Š., Hill, V., Recio-Blanco, A., et al. 2014, A&A, 572, A33
Mikolaitis, Š., Tautvaišienė, G., Gratton, R., Bragaglia, A., & Carretta, E. 2010, MNRAS, 407, 1866
Mikolaitis, Š., Tautvaišienė, G., Gratton, R., Bragaglia, A., & Carretta, E. 2011a, MNRAS, 413, 2199
Mikolaitis, Š., Tautvaišienė, G., Gratton, R., Bragaglia, A., & Carretta, E. 2011b, MNRAS, 416, 1092
Mikolaitis, Š., Tautvaišienė, G., Gratton, R., Bragaglia, A., & Carretta, E. 2012, A&A, 541, A137
Mishenina, T., Korotin, S., Carraro, G., Kovtyukh, V. V., & Yegorova, I. A. 2013, MNRAS, 433, 1436
Mishenina, T., Pignatari, M., Carraro, G., et al. 2015, MNRAS, 446, 3651
Nidever, D. L., Zasowski, G., Majewski, S. R., et al. 2012, ApJ, 755, L25
Nitz, D. E., Kunau, A. E., Wilson, K. L., & Lentz, L. R. 1999, ApJS, 122, 557
Overbeek, J. C., Friel, E. D., & Jacobson, H. R. 2016, ApJ, 824, 75
Pace, G., Danziger, J., Carraro, G., et al. 2010, A&A, 515, A28
Pagel, B. E. J., & Tautvaisiene, G. 1995, MNRAS, 276, 505
Pagel, B. E. J., & Tautvaisiene, G. 1997, MNRAS, 288, 108
Piskunov, N. E., Kupka, F., Ryabchikova, T. A., Weiss, W. W., & Jeffery, C. S. 1995, A&AS, 112, 525
Ramírez, I., & Allende Prieto C. 2011, ApJ, 743, 135
Reddy, A. B. S., & Lambert, D. L. 2015, MNRAS, 454, 1976
Reddy, A. B. S., & Lambert, D. L. 2017, ApJ, 845, 151
Reddy, A. B. S., Giridhar, S., & Lambert, D. L. 2012, MNRAS, 419, 1350
Reddy, A. B. S., Giridhar, S., & Lambert, D. L. 2013, MNRAS, 431, 3338
Reddy, A. B. S., Giridhar, S., & Lambert, D. L. 2015, MNRAS, 450, 4301
Salaris, M., Weiss, A., & Percival, S. M. 2004, A&A, 414, 163
Sampedro, L., Dias, W. S., Alfaro, E. J., Monteiro, H., & Molino, A. 2017, MNRAS, 470, 3937
Santos, N. C., Lovis, C., Pace, G., Melendez, J., & Naef, D. 2009, A&A, 493, 309
Santrich, O. J. K., Pereira, C. B., & Drake, N. A. 2013, A&A, 554, A2
Seggewiss, W. 1968, Mitteilungen der Astronomischen Gesellschaft Hamburg, 25, 172
Smiljanic, R., Gauderon, R., North, P., et al. 2009, A&A, 502, 267
Smiljanic, R., Romano, D., Bragaglia, A., et al. 2016, A&A, 589, A115
Smith, G. H. 1983, PASP, 95, 296
Sneden, C., Lawler, J. E., Cowan, J. J., Ivans, I. I., & Den Hartog E. A. 2009, ApJS, 182, 80
Sousa, S. G., Santos, N. C., Mayor, M., et al. 2008, A&A, 487, 373
Strassmeier, K. G., Weingrill, J., Granzer, T., et al. 2015, A&A, 580, A66
Tautvaišienė, G., Edvardsson, B., Tuominen, I., & Ilyin, I. 2000, A&A, 360, 499
Tautvaišienė, G., Edvardsson, B., Puzeras, E., & Ilyin, I. 2005, A&A, 431, 933
Tautvaišienė, G., Drazdauskas, A., Mikolaitis, Š, et al. 2015, A&A, 573, A55
Tautvaišienė, G., Drazdauskas, A., Bragaglia, A., Randich, S., &Ženovienė R. 2016, A&A, 595, A16
Thogersen, E. N., Friel, E. D., & Fallon, B. V. 1993, PASP, 105, 1253
Ting, Y.-S., De Silva, G. M., Freeman, K. C., & Parker, S. J. 2012, MNRAS, 427, 882
Tinsley, B. M. 1979, ApJ, 229, 1046
Tomkin, J., & Lambert, D. L. 1974, ApJ, 193, 631
Tomkin, J., Lambert, D. L., & Luck, R. E. 1975, ApJ, 199, 436
Travaglio, C., Gallino, R., Arnone, E., et al. 2004, ApJ, 601, 864
Twarog, B. A., Ashman, K. M., & Anthony-Twarog, B. J. 1997, AJ, 114, 2556
Škoda, P., Draper, P. W., Neves, M. C., Andrešič, D., & Jenness, T. 2014, Astron. Comput., 7, 108
Van der Swaelmen, M., Boffin, H. M. J., Jorissen, A., & Van Eck S. 2017, A&A, 597, A68
Wachlin, F. C., Miller Bertolami, M. M., & Althaus, L. G. 2011, A&A, 533, A139
Wachlin, F. C., Vauclair, S., & Althaus, L. G. 2014, A&A, 570, A58
Worley, C. C., Cottrell, P. L., Freeman, K. C., & Wylie-de Boer E. C. 2009, MNRAS, 400, 1039
Wyse, R. F. G., & Gilmore, G. 1988, AJ, 95, 1404
Yong, D., Carney, B. W., & Teixera de Almeida, M. L. 2005, AJ, 130, 597
Yong, D., Carney, B. W., & Friel, E. D. 2012, AJ, 144, 95
Zacharias, N., Finch, C. T., Girard, T. M., et al. 2013, AJ, 145, 44